DYNAMICS OF A SPRAY FORMED BY LAMINAR LIQUID JET IN MODULATED CROSSFLOW

V. Bodoc, A. Desclaux, P. Gajan, F. Simon, G. Illac

ONERA, Toulouse, France, virginel.bodoc@onera.fr

ABSTRACT

This paper deals with the study of the spray dynamics inside a turbojet engine injector in the frame work of thermo-acoustic instabilities comprehension and control. For that an experimental setup was developed at laboratory scale. It consists of a laminar water jet transversally injected into an oscillating air crossflow at ambient conditions. Phase Doppler Anemometry was used to determine the characteristics of crossflow and of the spray in terms of droplets velocity and concentration. The phase averaged technique was used to characterize the air velocity field and the spray oscillations during the excitation cycle. The results reveal the existence of velocity and concentration waves travelling behind the liquid jet. Coupling phenomena between the crossflow, the atomization of the liquid jet and the transport of droplets are observed, revealing different wave transport velocities. It was also proved that the spray dynamics is piloted either by the liquid column or by the crossflow oscillations.

KEYWORDS

TURBGOJET ENGINE, THERMO-ACOUSTIC INSTABILITIES, SPRAY DYNAMIC, MODULATED FLOW

NOMENCLATURE

q	momentum flux ratio
We	Weber number
V_j	jet initial velocity
d	nozzle diameter
U_0	airflow bulk velocity
V_j	liquid jet bulk velocity
U	longitudinal component of the velocity
V	transversal component of the velocity
χ	number of drops rate
ϕ	phase angle
N	number of droplets

INTRODUCTION

Turbojet combustor is predisposed to thermo-acoustic instabilities in which the unsteady behavior of the liquid fuel may play an important role (Apeloig et al., 2015). In the multipoint zone of the injector the atomization is based on the shearing of the liquid jet fuel. In steady conditions the liquid fuel is atomized and directly transported to the combustor. In presence of thermo-acoustic instabilities the fuel jet behavior may change with the airflow fluctuations and different atomization regimes may occur during the instability cycle. Hence, for high airflow rates the liquid jet penetration is very small and the jet reattaches the inner wall of the radial swirler producing a liquid film that is reatomized at the edge of the diffuser. For low airflow rates the fuel jet impinges the outer wall of the radial swirler forming a liquid film which is reatomized further downstream. These

regimes have different characteristic times due to the distinct mechanisms involved in the liquid atomization and transport from the injection point to the combustor.

Following Mashayek and Ashgriz (2011) the atomization processes involved in the liquid jet in crossflow can be divided into three main categories of primary break-up, column break-up and secondary break-up. The primary/surface break-up refers to the separation of droplets from the surface of the liquid jet. The column break-up refers to the disintegration of the liquid column as a whole in large parcels of liquid. The secondary break-up refers to the process that the separated droplets and parcels of liquid undergo after they are detached from the jet body.

Wu et al. (1997) studied by laser shadography the break-up process of liquid jets injected into subsonic steady crossflow. Different liquids and operating parameters were varied to provide a wide database. Results indicate that for high injection velocity the liquid jet penetrates far into the crossflow and exhibits surface break-up before the column breaks. Liquid column trajectories and the height of the column fracture point were found to be correlated by liquid/air momentum flux ratio (q) only. In addition, it was proved that the liquid column always breaks at the same streamwise location.

Sallam et al. (2004) performed a more in depth investigation of the break-up of laminar liquid jets in steady subsonic crossflow at normal temperature and pressure by pulsed shadography. From this analysis different characteristics were inferred: primary break-up regimes, conditions required for the onset of ligament and drop formation ligament and drop size along the liquid surface, drop velocity after break-up, rates of liquid break-up along the liquid surface, conditions required for the break-up of the liquid column as a whole and liquid column trajectories. The primary break-up process was found to be a function of the Weber number.

At this point it must be said that no much experimental data exist on droplets dynamics downstream the liquid jet for a steady crossflow. However, it was demonstrated by numerical simulation (Mashayek and Ashgriz, 2011) that air flow structures may be associated to the presence of the liquid jet and they play an important role in the drop dynamics.

Within a program to evaluate active control of combustion instabilities that involve acoustic/spray coupling, Anderson et al., (2001) performed an experimental investigation on a steady and modulated fuel jet in an unsteady crossflow. They observed that the spray distribution is affected by the modulation of the crossflow, especially faraway from the injection nozzle. Measurements by a laser extinction technique have shown that a phase lag appears for droplets further from the injection side wall, probably because of the sluggishness of more large droplets and transport delay.

Song and Lee (2015) presented experimental results on the response of spray formed by a kerosene jet injected in a modulated crossflow. The characterization of the spray shows that there exist little differences in the heights of the maximum pixel intensity trajectory for the non-oscillation and oscillating crossflow conditions. They suggested that the oscillating crossflow enhances the atomization process, results in smaller droplets and penetrates less into the flow.

For a better understanding of atomization and transport mechanisms involved within such injectors an experiment was developed at ONERA. Within this paper the characterization of the spray formed by liquid jet injected into oscillating airflow is presented. The setup consists in a laminar water jet transversally injected into an oscillating air crossflow at ambient conditions.

EXPERIMENTAL SETUP

A detailed description of the experimental setup was published previously (Bodoc et al., 2008). Only some basic elements will be included here for completeness. The left image from Figure 1 presents the test model. It is connected to the pneumatic loudspeaker through a 2 m long straight pipe having a 50X50 mm^2 square cross section. The overall pipe length downstream of the pneumatic loudspeaker and the excitation frequency were defined to obtain acoustic modes in the frequency range observed in combustion chambers (between 100 Hz to 600 Hz). The outlet liquid jet is placed close to a velocity antinode corresponding to high air velocity fluctuations.

The test model consists of three zones. The inlet zone, 100 mm long, has the same cross section as the upstream duct. It is followed by a convergent part ensuring a channel height reduction with a smooth transition without airflow separation. The third part, 110 mm long and rectangular cross section (20x50 mm^2), corresponds to the test section.

A liquid jet of water is injected vertically upwards in the symmetry plane of the test model. The injector nozzle is flush mounted with the wall and is placed 100 mm from the exit of the channel. Measured mass flow rate is used to calculate the jet initial velocity (V_j) at the nozzle exit. The injector internal geometry (right image in the figure) is adapted from (Wu et al., 1997) in order to guarantee a low turbulent jet.

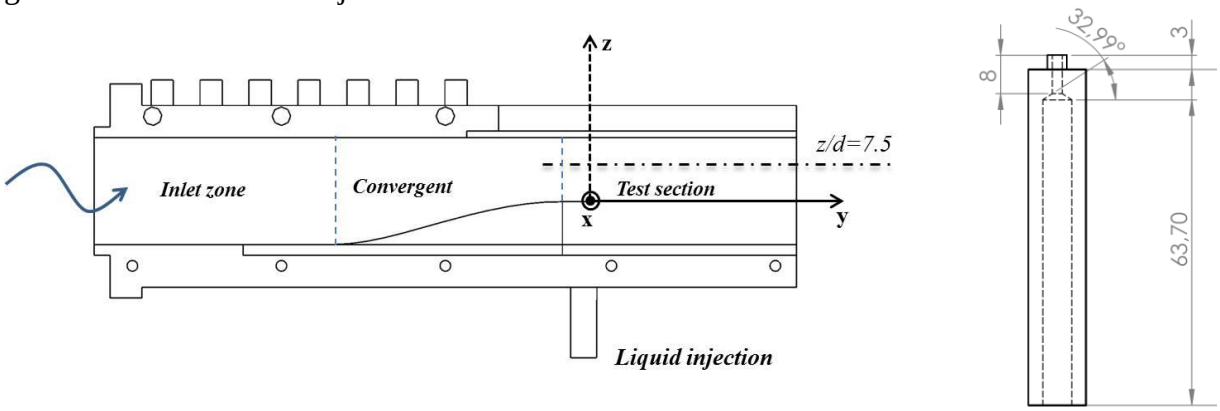

Figure 1: Experimental setup (left side image) and nozzle geometry (right side image)

For optical diagnostic, the lateral walls of the test section are made in Perpex and the top filming wall is realized in glass. A set of 7 microphone taps placed as in the image enables the acoustical characterization of the setup.

The characteristics of the water spray were measured in different locations at a dimensionless distance of z/d=7.5 from the bottom wall. The experimental conditions considered for this study are summarized in Table 1**Erreur ! Source du renvoi introuvable.**. The air and liquid velocities are chosen to reproduce the main flow phenomena encountered in aeronautical devices in working conditions (Apeloig et al., 2015). The momentum flux ration (7.8 for water experiments versus q~2.2 for engine conditions) and the height of the test channel were determined to allow the periodic impact of the liquid jet on the upper wall. The Weber number is different for water tests and engine conditions (~2260 versus ~160, respectively) but, following the regime maps of Wu et al. (1997) and Sallam et al. (2004), for both values of *We* the atomization process corresponds to the shear break-up regime.

Parameter	Values
Air flow rate [g/s]	79.8
Air bulk velocity [m/s]	66.65
Air temperature [K]	~290
Air pressure [bar]	~1
Test liquid	Water
Liquid temperature [K]	~290
Liquid velocity V_j[m/s]	6.15
Mean momentum flux ratio q [-]	7.8
Mean Weber number We [-]	136
Reynolds number of the air Re_{air} [-]	~21500
Reynolds number of the liquid jet [-]	~10000
Airflow modulation frequency [Hz]	177

Table 1. Experimental conditions

The characterization of the acoustical field, of the air crossflow in the absence of the liquid phase and the liquid jet trajectory were the main concerns of another publication (Bodoc et al., 2018). Within this paper the focus is on the spray behavior analysis using the Phase Doppler Anemometry (PDA) technique. To characterize the air velocity field and the spray oscillations during the excitation cycle, the PDA was triggered by the loudspeaker excitation signal and the measurements were made at 90 different phases with 4° increment. In general, the data rate ranges between 2300-6000 samples/s except very close to the liquid jet where it falls to 50 samples/s. As expected this is due to the presence of large, non-spherical liquid structures which are out of the PDA measurement range. At each measurement location 1 000 000 validated droplets were measured with typical validation rates in the range of 80-95%.

RESULTS AND DISCUSSIONS

Air flow characterization

The velocity distribution of the airflow in the symmetry plane was measured for both steady and modulated flow conditions using the same PDA method. Figure 2 shows the evolution of the velocity profile when the air flow is modulated by the loudspeaker at a constant frequency of 177 Hz. The abscissa axis corresponds to the air velocity while the ordinate axis corresponds to the distance from the bottom wall (x/d=0,y/d=0). Each profile corresponds to a different phase angle. In the central region of the duct (z/d>2) the velocity distribution is almost uniform and the velocity decreases towards the walls. For the different phases of the modulation the velocity values are almost identical beyond z/d=1, suggesting that the velocity distribution is maintained during modulation cycle even than the mean velocity fluctuates. The amplitude (in RMS values) of the modulation is measured to be 10% of the mean velocity at the modulation frequency.

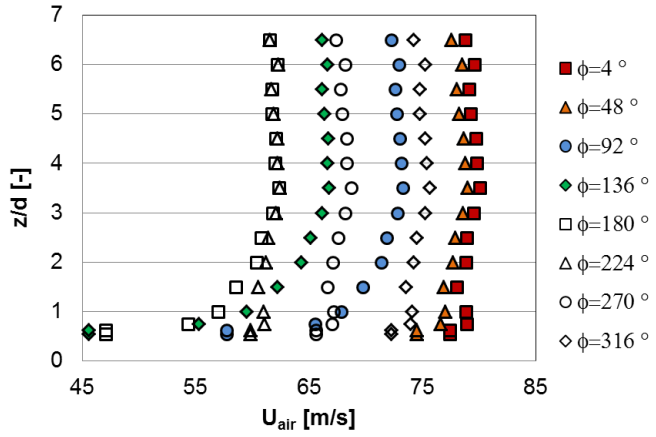

Figure 2 : The oscillation of the velocity profile when the air crossflow is modulated at 177 Hz. Measurements are performed at different phase angles

Characterization of liquid phase

Mean Behavior of the Spray

The evolution of the streamwise component of the droplets mean velocity is shown in Figure 3 (left side). The plotted values of velocity are expressed in dimensionless units after division by the airflow mean bulk velocity U_0. It shows that the droplets velocity increases continuously downstream in the flow. It reaches a maximum value just after the exit from the test channel and decreases further downstream due to the gas expansion. Nevertheless, due to their inertia, the droplet velocity does not reach the air velocity.

Right side image of Figure 3 shows the evolution of the vertical component of the droplets mean velocity. The plotted values are expressed in dimensionless units after division by the jet initial

velocity V_j. In the first part of the spray the vertical component of droplets velocity is much higher than the injection velocity. The "up-and-down" flapping of the liquid jet submitted to a modulated air crossflow could be the origin of this result. Downstream in the channel the vertical component of the velocity decreases for two reasons. On the one hand, away from the column jet the droplets are entrained by the gaseous crossflow. On the other hand the droplets with a high vertical velocity impinge the upper wall and disappear from the PDA statistics. At y/d~26 the vertical component of the velocity vanishes or becomes slightly negative. In the author's opinion the negative values of the velocity may be explained by the emergence of new droplets during the liquid jet impingement onto the upper wall. This hypothesis will be supported further downstream by the droplets size evolution but further investigations are needed for its full assessment.

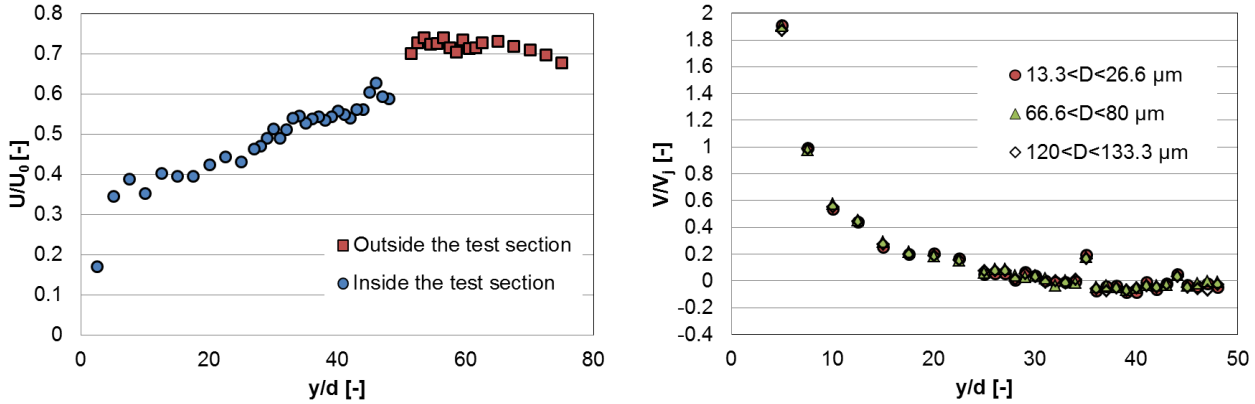

Figure 3: Evolution of the droplets longitudinal mean velocity (left image) and vertical mean velocity (right image). The vertical mean velocity is plotted for different classes of sizes.

Figure 4 shows the velocity profiles for droplets of different sizes. For the sake of simplification each histogram of sizes was described by only 10 classes of diameters. Each image of the figure shows the velocity evolution for five classes. Abscissa axis corresponds to the distance to the injection axis, while the ordinate axis corresponds to the drops longitudinal velocity expressed in dimensionless units. In general, the profiles show a monotone, linear evolution of velocity with the distance to the liquid jet. As expected, the velocity of small droplets increases faster than that of large droplets in reason of their high dynamic response. A particular behavior is observed for small droplets (0<D<40 µm). For y/d~26 their velocity increases quickly. This "jump" could be explained by the same phenomenon of droplets emergence from the wall. From the data plotted in Figure 4 the size of this new population of droplets that travels at higher velocity ranges from 0 to 40 µm.

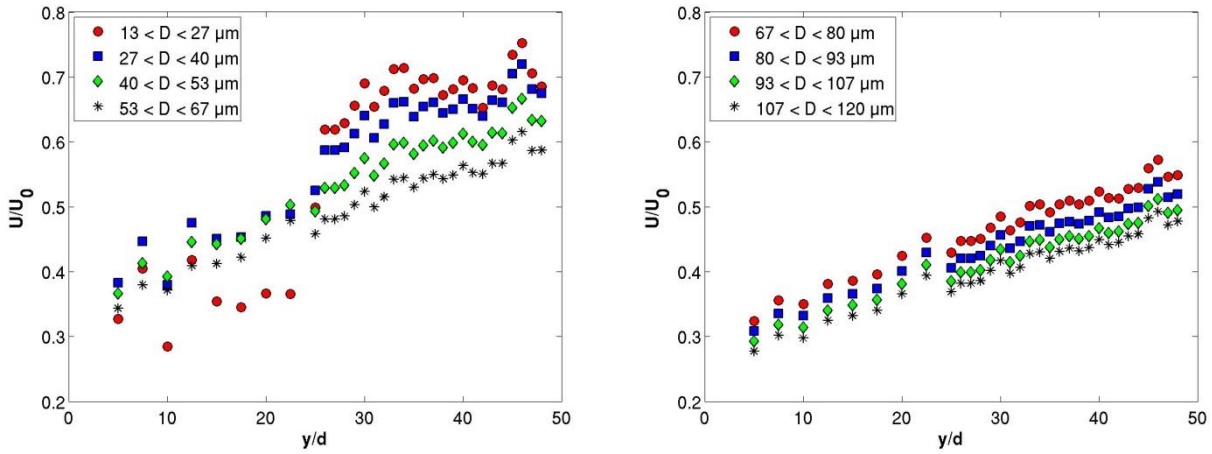

Figure 4 : Evolution of the mean longitudinal component of the droplets velocity

To confirm this hypothesis Figure 5 compares the droplet size distributions obtained for different longitudinal locations in the test section. It is obvious that the shape of the histogram changes for y/d>25 because of increase of number of drops with small sizes.

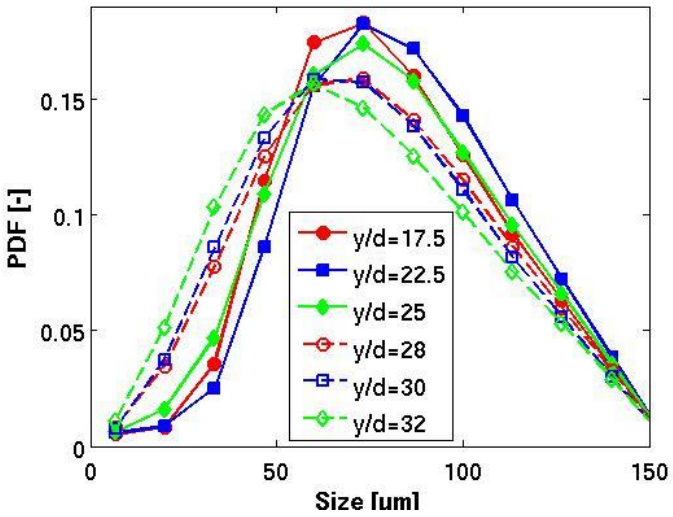

Figure 5 : Droplet size distribution at different locations downstream the injection axis

Figure 6 shows profiles of droplets longitudinal velocity fluctuations calculated as RMS values for different classes of sizes. Close to the liquid jet (y/d<26) the velocity fluctuations decrease with the same rate for all the droplets. This result suggests that the cycling nature of droplet velocity is mainly due to the jet column fluctuations. Further downstream (y/d>26), after reaching a minimal value that is different for each class of sizes, the velocity oscillations increase. The increasing rate is higher for the smallest droplets because of their smaller dynamic response time. This behavior suggests that, in this part of the channel, the cycling nature of droplets velocity is due to the crossflow fluctuations.

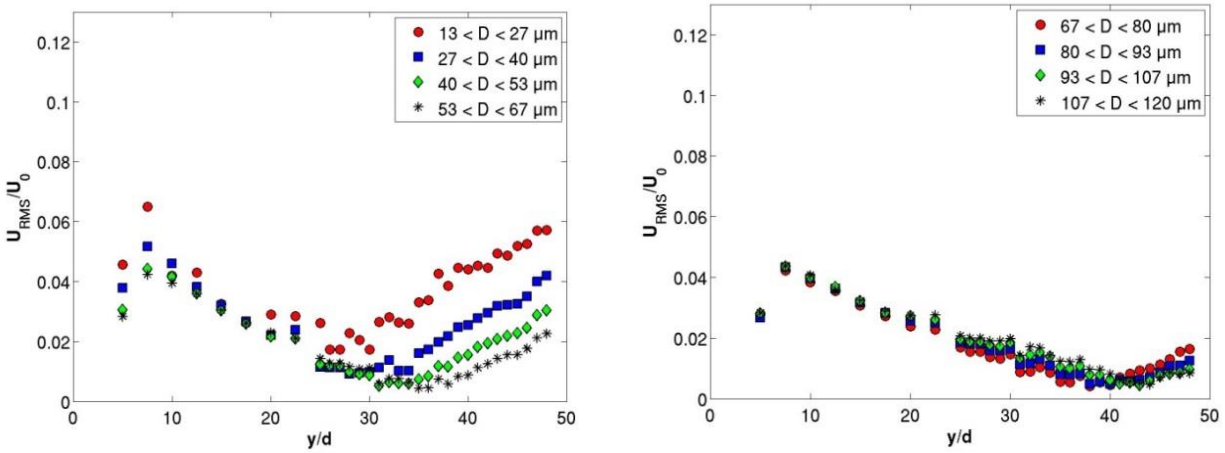

Figure 6 : Profiles of droplets longitudinal velocity fluctuations

Cyclic Behavior of the Spray

Following the analysis of PDA measurements independently of the crossflow fluctuations, the effect of the air modulation on droplets velocity and concentration is evaluated by a phase-averaged approach. A typical three-dimensional plotting of the droplets size distribution with respect to the excitation phase obtained in one location is shown in Figure 7. The color levels correspond to the longitudinal component of the droplets velocity. This figure shows that the excitation imposes an important variation of the number of droplets during the excitation period. The color mapping reveals that the maximum velocity zone is reached for the minimum drops population. Moreover,

for each phase angle, the maximum value of the longitudinal velocity does not correspond to the smallest droplets.

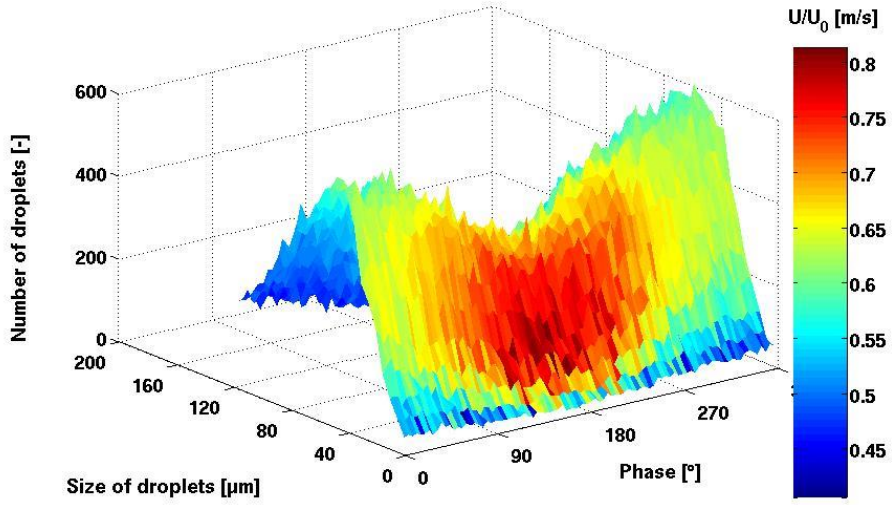

Figure 7 : Evolution of droplets size distribution during a pulsation cycle. The color levels correspond to the droplet longitudinal velocity

In the analysis of the cyclic behavior of the spray the number of droplets rate χ is introduced. This parameter that is representative to a droplet concentration is computed from the PDA measurements and corresponds to the number of droplets detected at a given phase angle $N(\phi)$ divided by the average number of droplets detected within the whole cycle N_T (overall number of droplets detected divided by the number of phase steps considered):

$$\chi(\phi) = \frac{N(\phi)}{N_T}$$

A cyclic phenomena observed at y/d=10 downstream the liquid jet is analyzed in Figure 8. The three profiles correspond to the droplets velocity (U/U_0), the number of drops rate (χ) and the droplets mean diameter (D10). Different phase delays are observed between the three signals. The minimum velocity corresponds to large droplets and droplet concentration. When compared with the air velocity signal (continuous black line) measured at y/d=0, it can be noticed that the highest presence of droplets corresponds to high crossflow velocity, and inversely, a low presence is obtained when low air velocity occurs.

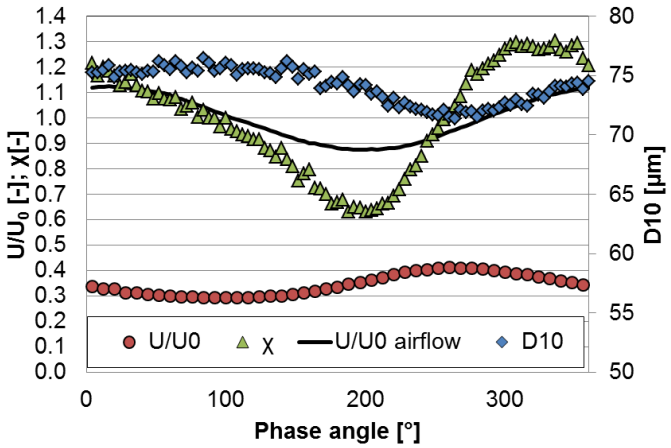

Figure 8 : Droplets velocity, concentration and size evolution during a modulation period (y/d=10)

Figure 9 shows velocity and concentration signals obtained at different distances from the injection axis. The left graph shows the existence of a velocity wave that shifts from one location to the next. This behavior corresponds to a convective phenomenon.

From the right graph is quite impossible to conclude on the presence of a concentration wave traveling downstream in the flow. If for some measurement locations (y/d=7.5 and y/d=10) the existence of such a wave is obvious, the shape of signals changes for the other locations. It is believed that this is due to the different atomization mechanisms involved: column break-up, shear stripping and secondary break-up, each of them occurring with difference phase shifts with respect to the crossflow oscillation. The simultaneous presence of all these mechanisms makes impossible the formation of a concentration wave at the crossflow frequency in the first part of the channel. However, such a concentration wave was identified for y/d>30. As demonstrated by Gajan et al. (2007) the mechanism that may explain the formation of this concentration wave away from the liquid column is the transport of droplets by the convective velocity wave.

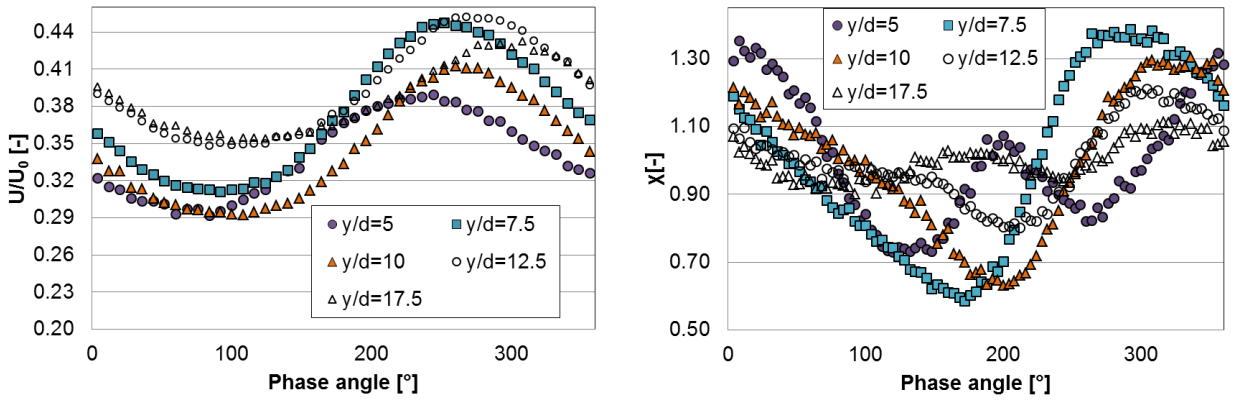

Figure 9 : Droplets velocity and concentration signals for different downstream locations

Figure 10 shows the evolution of the velocity wave phase delay for different classes of sizes. It was calculated with respect to the crossflow velocity signal measured on the injection axis. The horizontal axis corresponds to the measurement location while the vertical axis corresponds to the phase delay that lies between ±180°. Just after the atomization a large phase delay is measured between the crossflow modulation and the droplets velocity (superior to 180°). Because this value does not vary much with the size of droplets it is reasonable to affirm that the velocity oscillations of all droplets are coherent and related to the oscillation of the liquid jet. Downstream in the crossflow the phase delay increases monotonically suggesting the convection of the velocity wave.

For the region ranging from y/d=26 to y/d=30 a "jump" is observed in the phase delay profile. Because the jump location increases with the size of droplets, it is believed that this region corresponds to a "transition" region between the jet and crossflow nature of velocity oscillations. In fact, large droplets, due to their large momentum, keep their initial oscillation, due to the liquid jet flapping, in the first part of the test section and start to follow the crossflow oscillations only further in the channel. Because their transport time is different to the small droplets, in the first part of the channel the coherent movement of droplets is seriously affected.

The transition from one entrainment nature to another introduces an additional delay to the crossflow oscillation. To eliminate any ambiguity, in Figure 10 the curves with positive slopes have no physical meaning. Actually, they are just artefacts of the phase delay calculation algorithm when applied to non-sinusoidal signals. The same observation is valid for the next figure.

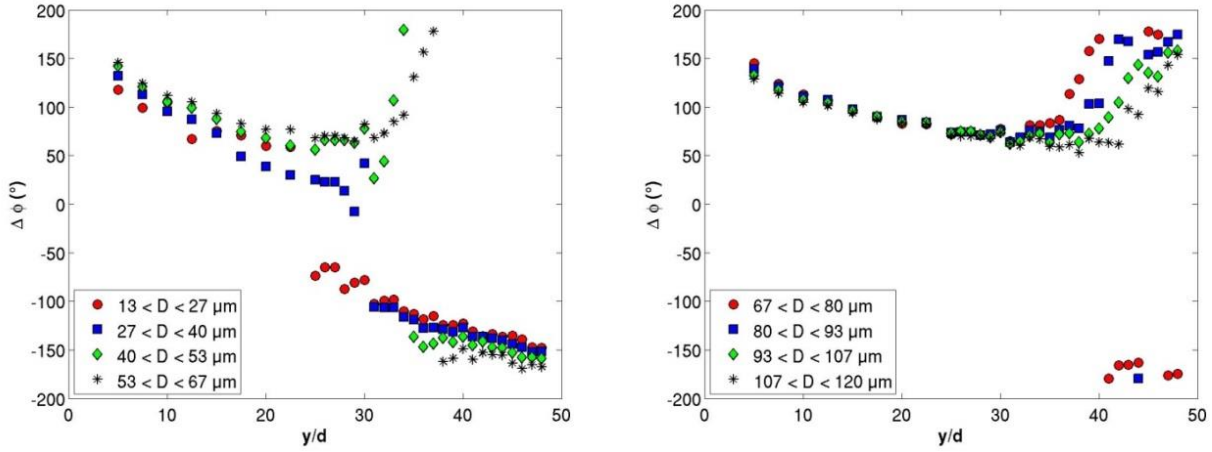

Figure 10: Evolution of the phase delay of droplets velocity wave.

Figure 11 shows the evolution of the phase shift of concentration wave with respect to the air velocity signal. For y/d<26 the measured values of phase delay do not have a physical meaning because the concentration wave is not yet formed. For y/d>26 the linear evolution of the phase delay for all the classes of size proves the formation of the concentration wave that is transported to the exit of the channel. From the slope of the curves the convection velocity may be calculated.

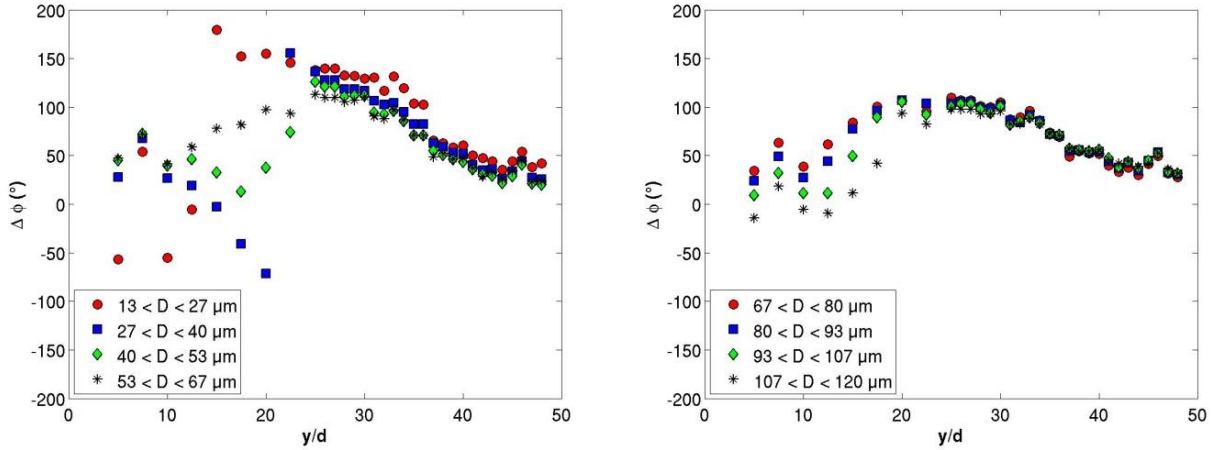

Figure 11: Evolution of the phase delay of droplets concentration wave.

CONCLUSIONS

Within this paper the behavior of a laminar liquid jet injected in a modulated crossflow was analyzed. The interest of this work is determined by the need to broaden the understanding on the atomization and transport mechanisms of the liquid fuel inside a turbomachinery injector in order to limit and/or control the thermo-acoustic instabilities.

A PDA/LDA method was applied to determine the characteristics of the gaseous flow and of the spray in terms of droplets size, velocity and concentration. The phase averaged technique was used to characterize the air velocity field and the spray oscillations during the excitation cycle.

The results reveal the existence of travelling velocity and concentration waves inside the test chamber. Coupling phenomena between the crossflow oscillations, atomization of the liquid jet and transport of droplets were observed. One of the main issues of this work is that behind the liquid jet the droplets dynamics is piloted by the oscillation of the liquid column. Further downstream the crossflow oscillations become the main pilot of droplets behavior. It was also observed that a concentration wave is not present just behind the liquid jet. The simultaneous presence of different

atomization mechanisms yields impossible the formation of such a wave. Nevertheless, this is possible further downstream while the droplets are piloted by the crossflow oscillations.

If it is obvious that the droplets velocity and concentration follow the oscillation of the air crossflow, the atomization of the liquid jet and interaction with the filming wall are complex processes. As an example, the spray impingement on the upper plate changes the size distribution of droplets with consequences on the velocity and concentration waves.

In order to identify the role of each atomization mechanism, this study needs to be broadened for additional operating conditions. Hence, a higher penetration of the liquid jet and larger modulation amplitude of the crossflow may further highlight the change of the atomization mechanism during one period of oscillation.

ACKNOWLEDGEMENTS

This research was supported by ONERA - The French Aerospace Lab.

REFERENCES

Anderson T.J., Proscia W., Cohen J.M., (2001), *Modulation of a liquid-fuel jet in an unsteady cross-flow*, Proceedings of ASME Turbo Expo 2001, New Orleans, USA

Apeloig J.M., d'Herbigny H.X., Simon F., Gajan P., Orain M., Roux S., (2015), *Liquid-Fuel Behavior in an Aeronautical Injector Submitted to Thermoacoustic Instabilities*, Journal of Propulsion and Power, 31(1), 309-319

Song J., Ramasubramanian C. and Lee J.G., (2013), *Response of liquid jet to modulated crossflow*, Proceedings of ASME Turbo Expo 2013, San Antonio, USA

Song J., Lee J.G., (2013), *Characterization of spray formed by liquid jet injected into oscillating air crossflow*, Proceedings of ASME Turbo Expo 2015, Montréal, Canada.

Sharma A., Lee J. G., (2018), *Dynamics of near-field and far-field spray formed by liquid jet in oscillating crossflow*, Atomization and Sprays, 28(1):1-21

Wu P. K., Kirkendall K. A., Fuller R. P. and Nejad A. S.,(1997) *Breakup process of liquid jets in subsonic crossflows*, Journal of Propulsion and Power, vol. 13, no. 1, pp. 64-73

Mashayek A., Ashgriz N., (2011), *Chapter 29 – Atomization of a Liquid Jet in Crossflow* In Handbook of Atomization and Sprays, Springer Science+Business Media, LLC .

Sallam K.A., Aalburg C., Faeth G.M., (2004), *Breakup of round nonturbulent liquid jets in gaseous crossflow*, AIAA journal, vol. 13, no. 1, pp. 64–73

Bodoc V., Descalux A., Gajan P., Simon F., Illac G.,(2018), *Characterization of confined liquid jet injected into oscillating air crossflow*, INCA Symposium, Paris 2017.

Gajan P., Strzelecki A., Platet B., Lecourt R., (2007), *Investigation of spray behavior downstream of an aeroengine injector with acoustic excitation*, Journal of Propulsion and Power, vol. 23, no. 2, pp.390-397